A Tailor-Made Deazaflavin-Mediated Recycling System for Artificial Nicotinamide Cofactor Biomimetics

Drenth, Jeroen; Yang, Guang; Paul, Caroline E.; Fraaije, Marco W.

DOI
10.1021/acscatal.1c03033

Publication date
2021

Document Version
Final published version

Published in
ACS Catalysis

ACS Catalysis

pubs.acs.org/acscatalysis

Research Article

A Tailor-Made Deazaflavin-Mediated Recycling System for Artificial Nicotinamide Cofactor Biomimetics

Jeroen Drenth,[§] Guang Yang,[§] Caroline E. Paul, and Marco W. Fraaije*

Cite This: *ACS Catal.* 2021, 11, 11561–11569

Read Online

ACCESS | Metrics & More | Article Recommendations | Supporting Information

ABSTRACT: Nicotinamide adenine dinucleotide (NAD) and its 2′-phosphorylated form NADP are crucial cofactors for a large array of biocatalytically important redox enzymes. Their high cost and relatively poor stability, however, make them less attractive electron mediators for industrial processes. Nicotinamide cofactor biomimetics (NCBs) are easily synthesized, are inexpensive, and are also generally more stable than their natural counterparts. A bottleneck for the application of these artificial hydride carriers is the lack of efficient cofactor recycling methods. Therefore, we engineered the thermostable F_{420}:NADPH oxidoreductase from *Thermobifida fusca* (*Tfu*-FNO), by structure-inspired site-directed mutagenesis, to accommodate the unnatural N1 substituents of eight NCBs. The extraordinarily low redox potential of the natural cofactor $F_{420}H_2$ was then exploited to reduce these NCBs. Wild-type enzyme had detectable activity toward all selected NCBs, with K_m values in the millimolar range and k_{cat} values ranging from 0.09 to 1.4 min^{-1}. Saturation mutagenesis at positions Gly-29 and Pro-89 resulted in mutants with up to 139 times higher catalytic efficiencies. Mutant G29W showed a k_{cat} value of 4.2 s^{-1} toward 1-benzyl-3-acetylpyridine (BAP^+), which is similar to the k_{cat} value for the natural substrate $NADP^+$. The best *Tfu*-FNO variants for a specific NCB were then used for the recycling of catalytic amounts of these nicotinamides in conversion experiments with the thermostable ene-reductase from *Thermus scotoductus* (*Ts*OYE). We were able to fully convert 10 mM ketoisophorone with BAP^+ within 16 h, using F_{420} or its artificial biomimetic FOP (FO-2′-phosphate) as an efficient electron mediator and glucose-6-phosphate as an electron donor. The generated toolbox of thermostable and NCB-dependent *Tfu*-FNO variants offers powerful cofactor regeneration biocatalysts for the reduction of several artificial nicotinamide biomimetics at both ambient and high temperatures. In fact, to our knowledge, this enzymatic method seems to be the best-performing NCB-recycling system for BNAH and BAPH thus far.

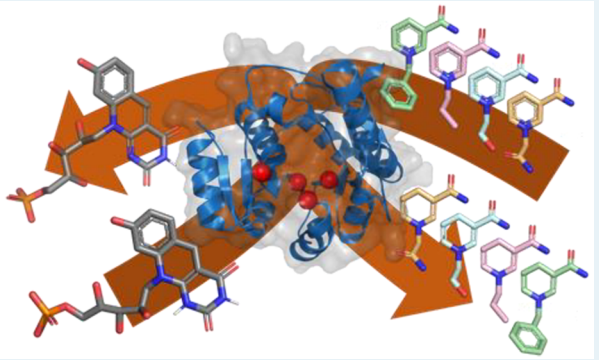

KEYWORDS: *deazaflavins, artificial cofactors, F_{420}, nicotinamide biomimetics, redox enzymology, enzymatic recycling system, enzyme engineering*

INTRODUCTION

An increased use of oxidoreductases for biocatalytic applications was seen in surveys of patent literature filed in the last two decades.[1−3] In fact, between 2000 and 2015, 68% of those patents were based on these enzymes.[3] Oxidoreductases make up nearly one-third of all enzymes,[4] and about half of them use a nicotinamide cofactor.[5] Nicotinamides and their *in vitro* performance are therefore of great importance to modern biocatalytic applications.

β-Nicotinamide adenine dinucleotide (NAD^+/NADH) and *β*-nicotinamide adenine dinucleotide 2′-phosphate ($NADP^+$/NADPH) are the two naturally occurring nicotinamide cofactor variants (see Figure 1A). The nicotinamide moiety (pyridine-3-carboxylic acid amide) is the redox-active part of the molecule, capable of accepting or donating a hydride. The adenosine diphosphate portion (ADP) serves as a recognition and anchoring point for enzymes. The presence or absence of the 2′-phosphate enables the cofactors to be discriminated by enzymes, while there are also enzymes that accept both nicotinamide cofactors.

The use of NAD(P)-dependent enzymes *in vitro* requires either a stoichiometric amount of the cofactor or a catalytic amount in combination with an *in situ* regeneration system. Although efficient enzymatic and nonenzymatic recycling systems already exist,[5,6] the stability and cost of NAD and especially NADP remain an issue for large-scale applications.[7,8] The ADP and ADP-2′-phosphate moieties of the natural nicotinamides are partially responsible for these issues but are not necessary for *in vitro* biocatalysis. Therefore, an array of

Received: July 6, 2021
Revised: August 22, 2021
Published: September 2, 2021

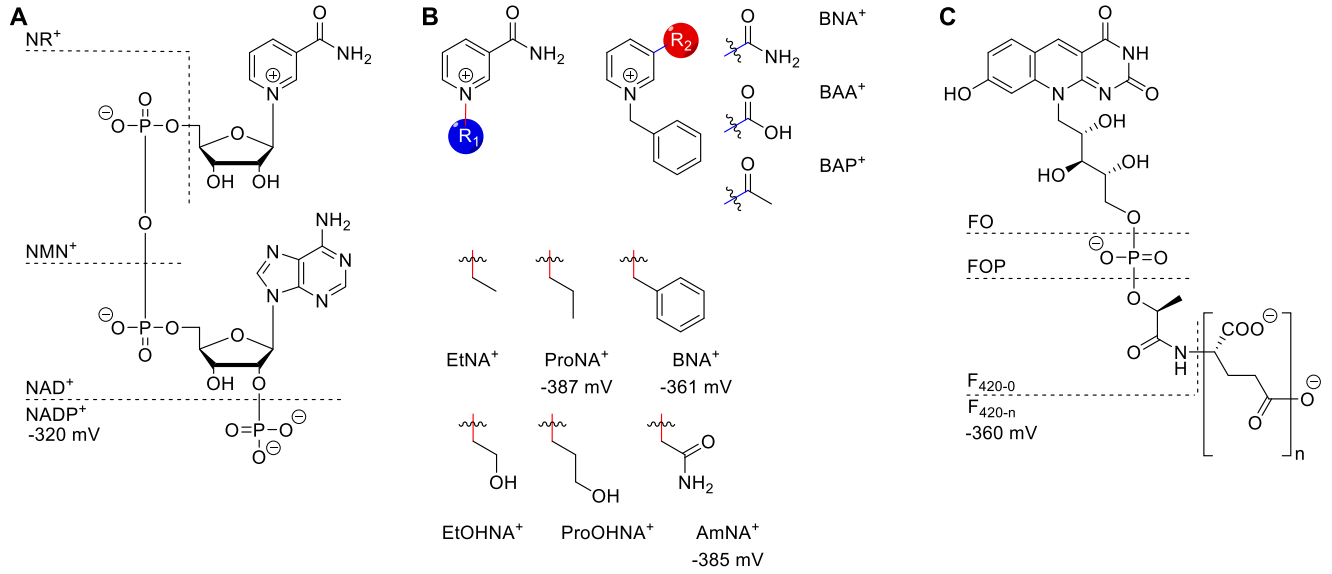

Figure 1. Nicotinamide and F_{420} cofactors: (A) The natural nicotinamides β-nicotinamide adenine dinucleotide (NAD) and β-nicotinamide adenine dinucleotide 2′-phosphate (NADP) and their redox-active natural precursors nicotinamide mononucleotide (NMN) and nicotinamide ribose (NR). (B) The artificial nicotinamide biomimetics that were investigated in this study. Their abbreviated names and redox potentials (when known) are shown below the structural formulas.[11] Their full names can be found in the Abbreviations. (C) The naturally occurring 5-deazaflavin cofactor F_{420} and its redox active natural precursor FO and the artificial biomimetic FOP.[12−14]

synthetic analogues known as nicotinamide cofactor biomimetics (NCBs) have been synthesized to overcome these problems. These relatively simple molecules are 1- and 3-substituted pyridines (see Figure 1B), which are easily synthesized from inexpensive, commercially available building blocks[9,10] and are generally more stable than NAD(P) under standard *in vitro* conditions.[7,9]

NCBs have been employed in several studies as reducing agents for oxidoreductases. Reduced 1-methylnicotinamide (MNAH) was the first of these synthetic cofactors that was successfully applied to reduce two redox enzymes, namely a DT diaphorase from Walker 256 rat carcinoma cells and a nitroreductase from *Escherichia coli*, with the same efficiency as NAD(P)H.[15,16] Thereafter, reduced 1-benzylnicotinamide (BNAH) and its *p*-methoxy analogue were used to reduce a mutant cytochrome P450 BM3 from *Bacillus megaterium* and P450cam from *Pseudomonas putida*, showing slightly lower specific activities of hydroxylation in comparison to NAD(P)H.[17] BNAH also works with 2-hydroxybiphenyl 3-monooxygenase (HbpA) from *Pseudomonas azelaica* HBP1,[18] with 3-hydroxybenzoate 6-hydroxylase (3HB6H) from *Rhodococcus jostii* RHA1, *p*-hydroxybenzoate hydroxylase (PHBH) from *Pseudomonas fluorescens*, and salicylate hydroxylase (SalH) from *P. putida*[19] and even improved the dye-degrading activity of the oxygen-insensitive azoreductase (AzoRo) from *Rhodococcus opacus* 1CP.[20] Several reduced NCBs were used on ene-reductases from the old yellow enzyme family (OYE), with varying activities between different OYE−NCB combinations.[21−25] In several cases the nicotinamide biomimetics outperformed the native cofactors NADH and NADPH.[21−23] Alcohol dehydrogenases, however, generally show no or very low activity toward NCBs, apart from horse liver ADH, which showed activity with BNAH as a hydride donor.[26−28] Their greater stability, lower cost, and sometimes enhanced performance with oxidoreductases make them lucrative alternatives for (NAD(P)).

Although these NCBs are significantly cheaper than their natural counterparts, stoichiometric addition of reduced NCB would still not be economically feasible. Therefore, several *in situ* recycling methods have been developed over the past few years. Two enzymatic recycling methods have been reported for the oxidation of reduced NCBs: namely a hydrogen peroxide driven myoglobin system for BNAH and the water-forming NADH oxidase from *Lactobacillus pentosus* for MNAH and BNAH.[29,30] Recycling reduced NCBs is considerably more challenging, due to their low redox potentials. The most popular recycling method for reduced NCBs, thus far, uses the formate-driven organometallic rhodium catalyst pentamethylcyclopentadienyl rhodium bipyridine, $[Cp^*Rh(bpy)(H_2O)]^{2+}$,[31] which has been used in several studies.[17,18,22,26,27] Two studies, however, have reported low initial activity and mutual inactivation of the organometallic catalyst and the enzyme, which form major bottlenecks for biocatalysis.[18,32] Several attempts to overcome these problems were reported, such as the use of different counterions for the rhodium catalyst,[17,26] catalyst separation,[33] carbon-nanodot-sensitized regeneration systems,[34] and artificial metalloenzymes that were based on streptavidin variants with biotinylated iridium catalysts.[35] To our knowledge, two studies have investigated enzymatic recycling systems of reduced NCBs. The two enzymes are an engineered 6-phosphogluconate dehydrogenase from *Thermotoga maritima* and an engineered glucose dehydrogenase from *Sulfolobus solfataricus* (*Ss*GDH).[36,37] Unfortunately, these recycling systems still have low catalytic efficiencies. The low catalytic activity might be caused by two separate, yet equally important, factors: (1) the poor structural complementarity between the 1-substituents of the NCBs and the enzyme scaffold and (2) the incompatibility of the low redox potentials of NCBs with most natural redox systems. The naturally occurring redox cofactor F_{420} (see Figure 1C), found in many archaea and actinobacteria, has an extremely low redox potential of −360 mV, which is close to the potentials of most NCBs.[11−13,38,39] Some organisms use

https://doi.org/10.1021/acscatal.1c03033
ACS Catal. 2021, 11, 11561−11569

F_{420}:NADPH oxidoreductases to catalyze the reversible hydride transfer between F_{420} and the natural nicotinamide NADPH. Therefore, these enzymes may form effective recycling systems for reduced NCBs, harnessing the strong reducing power of F_{420}.

Herein we describe the engineering of the thermostable F_{420}:NADPH oxidoreductase from *Thermobifida fusca* (*Tfu*-FNO)[40] to efficiently reduce a selection of NCBs (see Figure 1B). Structure-guided site-directed mutagenesis was used to make variants that better accommodate NCBs. These variants were then screened for improved activity toward selected NCBs, and the best mutants were further characterized with steady-state kinetics. The best *Tfu*-FNO variants for a given biomimetic were then used as recycling systems in conversion experiments with the ene-reductase from *Thermus scotoductus* (*Ts*OYE), using glucose-6-phosphate as a sacrificial electron donor. Also the artificial deazaflavin biomimetic FOP[14] (see Figure 1C) was employed as an equally efficient electron mediator, demonstrating that engineered FNO enables regeneration of catalytic amounts of reduced NCBs through the use of a catalytic amount of either F_{420} or an artificial deazaflavin biomimetic. In fact, this study presents the first mutagenesis study on an F_{420}-dependent enzyme for biocatalytic purposes, resulting in an efficient recycling system for a broad selection of NCBs at ambient and elevated temperatures.

MATERIALS AND METHODS

Materials. All chemicals and mutagenic primers were purchased from Sigma-Aldrich (Merck; St. Louis, MO, USA), unless stated otherwise. The natural nicotinamides NMN^+, NR^+, $NADP^+$ and NADPH were obtained from Sigma-Aldrich, and all artificial nicotinamide biomimetics were synthesized as described previously by Norris et al. and Knox et al.[9,10] Ligase and restriction endonucleases, as well as the bacterial expression and cloning strains *E. coli* NEB 10-beta, BL21 (DE3), and C41 (DE3), were obtained from New England Biolabs (NEB, Ipswich, MA, USA). PfuUltra Hotstart PCR Mastermix (Agilent Technologies) was used for mutagenic PCR (QuikChange). Plasmid DNA was isolated using the QIAprep Miniprep Kit, and PCR products were purified with the QIAquick PCR Purification Kit (Qiagen, Valencia, CA, US.A). F_{420} was isolated from *Mycobacterium smegmatis* mc^2 4517, as described by Bashiri et al. and Isabelle et al.[41,42] FOP was synthesized as previously described by Drenth et al.[14]

Expression and Purification of F_{420}-Dependent Enzymes. The F_{420}:NADPH oxidoreductase from *T. fusca* (*Tfu*-FNO) was expressed and purified as previously described by Kumar et al.[40] The F_{420}-dependent glucose-6-phosphate dehydrogenase from *R. jostii* RHA1 (FGD-RHA1) and the F_{420}-dependent sugar-6-phosphate dehydrogenase from *Cryptosporangium arvum* (FSD-Cryar) were expressed and purified as *N*-terminally SUMO-fused proteins, as previously described by Nguyen et al.[43] and Mascotti et al.,[44] respectively. The same plasmid constructs and expression strains were used as in the aforementioned literature.

***Ts*OYE Expression and Purification.** The thermostable ene-reductase from *T. scotoductus* (*Ts*OYE) was expressed and purified as previously described by Knaus et al. and Opperman et al.[22,45] with the following exceptions: *Ts*OYE was heat-purified at 70 °C for 90 min, saturated with FMN, desalted (PD10), concentrated (Amicon 10 kDa), and stored in 20 mM MOPS-NaOH pH 7.0.

***Tfu*-FNO Mutagenesis.** Site-directed mutagenesis was performed on the *Tfu*-FNO gene with the use of mutagenic primers, using the QuikChange mutagenesis kit (Stratagene), following the procedure of the manufacturer. Primers were designed with the Agilent QuikChange primer design tool (http://www.genomics.agilent.com/primerDesignProgram.jsp). The primers used are given in Table S1. Sequencing was performed at GATC/Eurofins Genomics (Konstanz, Germany). The plasmids were transformed into calcium chloride chemically competent *E. coli* NEB 10-beta for plasmid amplification and protein expression, using standard protocols.

Steady-State Activity Assays and Mutant Activity Screens. Steady-state parameters for the activity of wild-type and mutant *Tfu*-FNO variants toward NCBs were obtained by a spectrophotometric assay. The measurements were performed at 25 °C by adding 0.1−5 μM enzyme to 50 mM Tris-HCl, 100 mM NaCl, and 3% (v/v) DMSO at pH 8.0 with a constant $F_{420}H_2$ concentration of 40 μM and varying concentrations of NCBs between 0.1 and 250 mM. The absorbance at 400 nm was followed with time, and the observed slopes (k_{obs}) were calculated with $\varepsilon_{400}(F_{420})$ = 25.7 mM^{-1} cm^{-1}. All experiments were performed in triplicate. The k_{obs} values were plotted against de NCB concentration, and the data were fitted to the Michaelis−Menten equation (eq 1) or the Michaelis−Menten equation with substrate inhibition (eq 2) by nonlinear regression, using GraphPad Prism v. 6.0 (GraphPad Software Inc., La Jolla, CA, USA).

$$k_{obs} = \frac{k_{cat}[S]}{K_m + [S]} \quad (1)$$

$$k_{obs} = \frac{k_{cat}[S]}{K_m + [S]\left(1 + \frac{[S]}{K_i}\right)} \quad (2)$$

$F_{420}H_2$ was prepared by incubating 400 μM F_{420} with 10 μM FGD-RHA1 and 5 mM glucose-6-phosphate in 50 mM Tris-HCl at pH 8.0, until the yellow color disappeared. Then, the mixture was passed through an Amicon Ultra 0.5 mL centrifugal filter, with a 10 kDa molecular weight cutoff. The filtrate, containing 400 μM $F_{420}H_2$, was then immediately used for a spectrophotometric assay.

The mutant activities toward certain NCBs were screened at 25 °C by adding 1 μM enzyme to 50 mM Tris-HCl, 100 mM NaCl, and 3% (v/v) DMSO at pH 8.0, with 40 μM $F_{420}H_2$ and either 1 or 40 mM NCB. The absorbance at 400 nm was followed with time, and the observed initial slopes (k_{obs}) were calculated with $\varepsilon_{400}(F_{420})$ = 25.7 mM^{-1} cm^{-1}. All experiments were performed in duplicate. For the best-performing mutants this activity assay was also performed at 50 °C in triplicate.

Conversion Experiments. The reaction mixture, with a total volume of 500 μL, contained 50 mM Tris-HCl, 100 mM NaCl, and 3% (v/v) DMSO at pH 8.0 supplemented with 10 mM 2,6,6-trimethyl-2-cyclohexene-1,4-dione (ketoisophorone), 400 μM FOP or 100 μM F_{420}, 1.0 mM NCB (in the oxidized form), 5 μM *Ts*OYE, 5 μM *Tfu*-FNO, 10 μM FSD-Cryar, and 50 mM glucose-6-phosphate. The reactions were performed in closed 2 mL glass vials in the dark at 30 °C and 135 rpm for 3−24 h. The reaction was quenched by adding 100 μL of the mixture to 400 μL of acetonitrile and then incubated on ice for 5 min. This mixture was spun down at 8000*g* in a table-top centrifuge at 4 °C, and 10 μL of the supernatant was used for analysis on an HPLC instrument. The depletion of substrate was analyzed at 240 nm, using an

https://doi.org/10.1021/acscatal.1c03033
ACS Catal. 2021, 11, 11561−11569

Table 1. Steady-state Kinetic Parameters for Wild-Type Tfu-FNO and Selected Tfu-FNO G29X and P89X Variants toward Selected NCBs[a]

NCB	variant	k_{cat} (min^{-1})	K_m (mM)	k_{cat}/K_m (s^{-1} M^{-1})	$(k_{cat}/K_m)_{mutant}/(k_{cat}/K_m)_{wt}$
$AmNA^+$	wt	1.4 ± 0.07	12 ± 1.7	1.9 ± 0.29	
	G29S	9.6 ± 0.56	18 ± 2.5	8.8 ± 1.3	4.6 ± 0.98
	G29Y	3.2 ± 0.23	23 ± 3.5	2.3 ± 0.39	1.2 ± 0.28
	P89H	2.5 ± 0.21	14 ± 3.0	3.0 ± 0.69	1.6 ± 0.44
$EtOHNA^+$	wt	1.4 ± 0.06	20 ± 2.5	1.2 ± 0.15	
	G29Y	6.2 ± 0.58	23 ± 4.7	4.5 ± 1.0	3.8 ± 0.96
	P89H	2.9 ± 0.22	20 ± 3.3	2.4 ± 0.44	2.0 ± 0.44
	P89Y	5.0 ± 0.63	33 ± 9.2	2.5 ± 0.77	2.1 ± 0.69
$ProOHNA^+$	wt	0.25 ± 0.013	25 ± 3.0	0.17 ± 0.022	
	P89Y	0.71 ± 0.096	35 ± 10	0.34 ± 0.11	2.0 ± 0.7
$EtNA^+$	wt	0.44 ± 0.01	25 ± 1.4	0.29 ± 0.018	
$ProNA^+$	wt	0.09 ± 0.007	10 ± 2.8	0.15 ± 0.044	
	G29L	0.36 ± 0.057	18 ± 7.9	0.33 ± 0.16	2.2 ± 1.3
	P89H	0.27 ± 0.026	5.7 ± 1.9	0.79 ± 0.27	5.3 ± 2.4
	P89L	0.44 ± 0.048	27 ± 6.9	0.27 ± 0.075	1.8 ± 0.73
	P89Y	0.59 ± 0.11	35 ± 14	0.28 ± 0.12	1.9 ± 0.97
BNA^+	wt	0.27 ± 0.01	6.4 ± 0.60	0.70 ± 0.071	
	G29W	25 ± 1.1	4.3 ± 0.68	97 ± 15	139 ± 26
	G29Y	8.7 ± 0.64	9.5 ± 2.0	15 ± 3.4	21 ± 5.3
BAP^+	G29W	252 ± 14	7.4 ± 1.2	568 ± 97	
BAA^+	G29W	NA	NA	NA	

[a]The measurements were performed at 25 °C by adding 0.1−5 μM enzyme to 50 mM Tris-HCl, 100 mM NaCl, and 3% (v/v) DMSO at pH 8.0 with a constant $F_{420}H_2$ concentration of 40 μM and varying concentrations of NCBs between 0.1 and 250 mM. Absorbance traces over time were measured and fitted to the Michaelis−Menten model. Values are means from three independent measurements ± standard deviations. NA: not active. The corresponding Michaelis−Menten plots are shown in Figures S6 and S7 of the supporting information.

isocratic mobile phase of 60/40 water/acetonitrile on an Alltech Alltime HP C18 5 μ, 250 mm column.

RESULTS

***Tfu*-FNO Wild-Type Activity toward Selected NCBs.** The thermostable F_{420}:NADPH oxidoreductase from *T. fusca* (*Tfu*-FNO) was expressed and purified as described previously.[40] Then, the activity of *Tfu*-FNO for a selection of nicotinamide biomimetics (NCBs; see Figure 1B) was assessed spectrophotometrically. First, the optimal pH for NCB reduction was investigated by reducing 40 mM BNA^+ and $AmNA^+$ at pH 6−8. The optimal pH was determined to be 8 (Figure S9), which is the same as the previously published optimal pH for $NADP^+$ reduction.[40] Steady-state kinetic parameters were measured by varying the concentration of the NCBs, while a constant, saturating $F_{420}H_2$ concentration was maintained. The initial slopes of absorbance increase at 400 nm were measured, and the observed rates (k_{obs}) were calculated using ε_{400} = 25.7 mM^{-1} cm^{-1}. The observed rates were plotted against the cofactor concentration and fitted to the Michaelis−Menten model, with and without substrate inhibition (eqs 1 and 2, respectively). The resulting steady-state parameters are shown in Table 1. The Michaelis−Menten curves are shown in Figures S1 and S2. All tested biomimetics had detectable activity that could be fitted to the Michaelis−Menten models, with and without substrate inhibition. All compounds showed substrate inhibition at high concentrations (>40 mM). All K_m values were in the millimolar range, with the lowest value being for BNA^+ (6.4 mM) and the highest for $ProOHNA^+$ and $EtNA^+$ (25 mM). The k_{cat} values span from 0.09 min^{-1} for $ProNA^+$ to 1.4 min^{-1} for $AmNA^+$ and $EtOHNA^+$. This shows that wild-type *Tfu*-FNO has a very high specificity for $NADP^+$, as this native cosubstrate has a k_{cat} value of 4.9 s^{-1} and a K_m value of 1.1 μM.[40]

***Tfu*-FNO Mutagenesis.** Structure-guided site-directed mutagenesis was performed on *Tfu*-FNO, in order to improve the catalytic efficiency toward the nicotinamide biomimetics. The crystal structure of *Tfu*-FNO (PDB ID: 5N2I), with cocrystallized $NADP^+$, was used to identify sites for mutagenesis. Glycine-29, proline-89, alanine-87, and valine-113 were chosen as sites for mutagenesis, as these residues are in close proximity to the ribose moiety of $NADP^+$, which is substituted by small, similarly sized substituents in NCBs. Mutants A87S, V113S, G29X, and P89X were created with QuikChange-PCR, where X stands for F, H, I, L, M, N, Q, S, V, W, and Y. Single point mutations were introduced and screened for their activity toward the NCBs. All mutant FNOs had expression levels similar to that of wild type. Also, their apparent melting temperature, as measured by the Thermo-Fluor assay, did not change (data not shown), which is ideal for high-temperature conversion.

Mutant Activity Screens and Subsequent Steady-State Activity Measurements. The engineered *Tfu*-FNO variants G29X and P89X, harboring a single point mutation, were screened for their activity toward the different NCBs. The G29X and P89X mutants with a polar amino acid side chain (H, N, Q, S, and Y) were tested for their activity toward $EtOHNA^+$, $ProOHNA^+$, and $AmNA^+$, as these have a compatible polar N1 substituent. Similarly, G29X and P89X with apolar amino acid side chains (F, H, I, L, M, V, W, and Y) were tested for their activity with $EtNA^+$, $ProNA^+$, and BNA^+, which have apolar N1 substituents. The mutants were screened in 96-well format with a constant, saturating $F_{420}H_2$ concentration and an NCB concentration of either 1 or 40 mM. All mutants were also screened for their activity toward

https://doi.org/10.1021/acscatal.1c03033
ACS Catal. 2021, 11, 11561−11569

Scheme 1. TsOYE-Catalyzed Reduction of Ketoisophorone (2,6,6-Trimethyl-2-cyclohexene-1,4-dione; 2a) by NCBs[a]

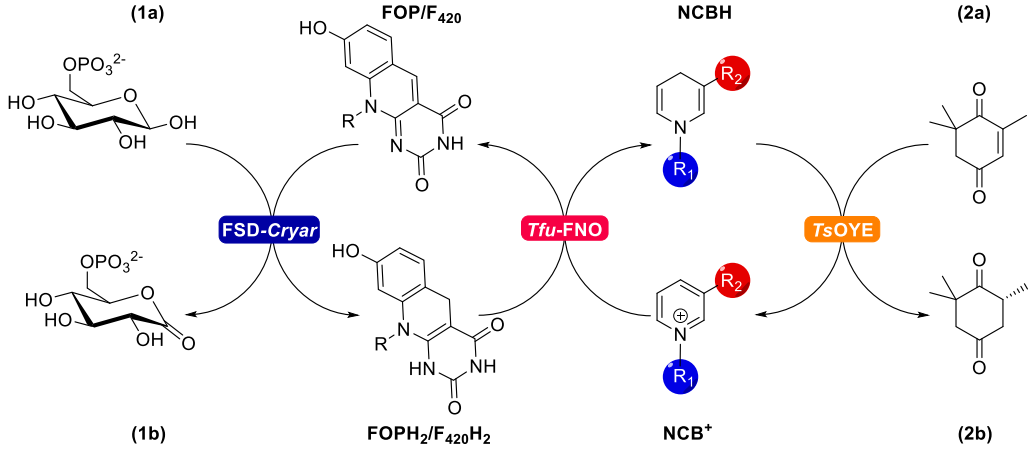

[a]Glucose-6-phosphate (**1a**) is used as a sacrificial electron donor for the reduction of F_{420} or FOP, as catalyzed by FSD-Cryar. Reduced F_{420}/FOP can then efficiently reduce several NCBs for the formation of the chiral product.

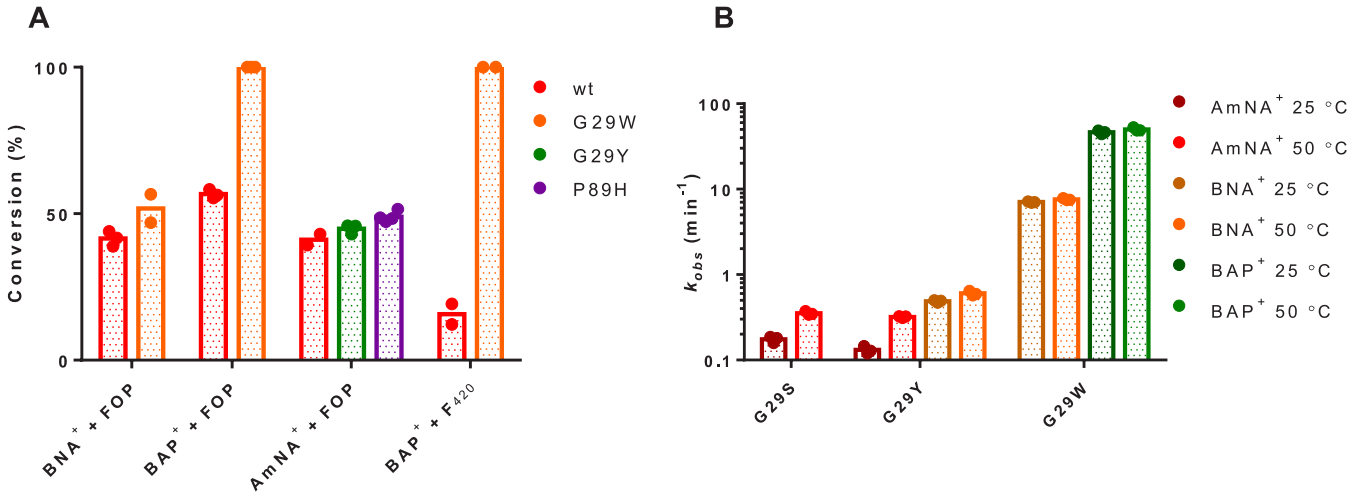

Figure 2. (A) *Ts*OYE-catalyzed conversion of 10 mM ketoisophorone, using 1 mM NCB, 100 μM F_{420} or 400 μM FOP, and glucose-6-phosphate as a sacrificial electron donor after 16 h at 30 °C. (B) Activity of selected Tfu-FNO variants toward 5 mM of nicotinamide biomimetic at either 25 or 50 °C. Bars represent average values of individual data points, which are represented by dots.

nicotinamide ribose (NR) and nicotinamide mononucleotide (NMN), which are the redox-active natural precursors of NAD(P). Figures S3–S5 in the Supporting Information summarize the results. No mutant was found with a significantly higher activity toward $EtNA^+$, NR^+, or NMN^+ in comparison with the wild-type enzyme. All other NCBs had at least one *Tfu*-FNO variant with significantly increased reduction rates. The kinetic parameters of these hits were then characterized spectrophotometrically, as was done before with wild-type *Tfu*-FNO. For 1-aminoethylnicotinamide ($AmNA^+$), variants G29S, G29Y, and P89H were identified as hits and indeed showed higher k_{cat} values in comparison to wild-type *Tfu*-FNO. The same trend was seen with G29Y, P89H, and P89Y for 1-hydroxyethylnicotinamide ($EtOHNA^+$), P89Y for 1-hydroxypropylnicotinamide ($ProOHNA^+$), and G29L, P89L, and P89Y for 1-propylnicotinamide ($ProNA^+$), where the mutants show a significant increase in maximum velocity of up to 7 times that of wild type *Tfu*-FNO. Mutants G29Y and G29W had an even more dramatic increase in activity toward 1-benzylnicotinamide (BNA^+), with 32 and 93 times higher reduction rates in comparison to wild type, respectively. The K_m value, however, hardly changed. Thus, most mutations do not seem to affect the overall binding affinity of these NCBs, but—probably—do induce subtle changes in the binding conformation that lead to more efficient hydride transfer.

Variant G29W, the variant with 139 times higher catalytic efficiency toward BNA^+ in comparison to wild type, was also tested for its activity toward 1-benzylnicotinic acid (BAA^+) and 1-benzyl-3-acetylpyridine (BAP^+), as both of them have the same N1 substituent. Although no apparent activity could be measured for BAA^+, profound activity was observed for BAP^+, with a k_{cat} value of 4.2 s^{-1} (252 min^{-1}). This maximum velocity is very similar to that of wild type toward its natural substrate $NADP^+$, which is 4.9 s^{-1}. The aforementioned results show that G29S, G29Y, P89H, and especially G29W could serve as effective recycling agents for AmNAH, BNAH, and BAPH.

Double mutants G29S/P89H, G29Y/P89H, and G29Y/P89Y were made for $AmNA^+$, $EtOHNA^+$, and $ProOHNA^+$, where hits in activity increase for positions 29 and 89 were both seen. These double mutants were screened in a 96-well format for their activity toward 1 mM $AmNA^+$, $EtOHNA^+$,

https://doi.org/10.1021/acscatal.1c03033
ACS Catal. 2021, 11, 11561−11569

ProOHNA$^+$, NR$^+$, and NMN$^+$. Unfortunately, none of these mutants showed better activity in comparison to the single mutants or wild type. Double mutants with two large, aromatic side chains might form steric clashes with the NCB or with their surroundings, therefore abolishing the NCB reduction activity.

The activity of the single mutants was also tested for the native substrate NADP$^+$ (see Table S2). Most mutations significantly decrease the activity toward NADP$^+$ but do not completely inhibit the enzyme for this cosubstrate. Adding mutations in the 2′-phosphate binding site, as was previously done by Kumar et al., might completely abolish NADP$^+$-reduction activity.[40] These *Tfu*-FNO variants might then be used for biorthogonal pathways that use NCBs and are not affected by the presence of NAD(P).

***Tfu*-FNO Variants as NCB-Recycling Systems for *Ts*OYE-Mediated Conversions.** *Ts*OYE is known to efficiently hydrogenate ketoisophorone (2,6,6-trimethyl-2-cyclohexene-1,4-dione) to form the chiral product (*R*)-2,2,6-trimethylcyclohexane-1,4-dione with high ee values of 94−97%, when several NCBs as more efficient electron donors in comparison to NADPH are used.[21,22] The *Tfu*-FNO variants G29Y, G29W, and P89H, which showed high activity toward AmNA$^+$, BNA$^+$, and BAP$^+$, were selected for use in conversion experiments as recycling catalysts for these NCBs. A catalytic amount of 1 mM oxidized NCB was used for the *Ts*OYE-catalyzed reduction of 10 mM ketoisophorone at 30 °C. F_{420} (100 μM) or FOP (400 μM) was used as an electron mediator, and glucose-6-phosphate was used as a sacrificial electron donor to fuel the reduction of NCBs through the action of the deazaflavin-dependent glucose-6-phosphate dehydrogenase FSD-Cryar (see Scheme 1). Reaction mixtures that contained *Tfu*-FNO G29W and P89H, in combination with BNA$^+$ or AmNA$^+$ as their respective nicotinamides, converted 5 mM of the substrate within 16 h of incubation. Mixtures containing the combination of G29W with the artificial nicotinamide BAP$^+$ even showed full conversion of 10 mM ketoisophorone within 16 h (see Figure 2A). Therefore, we could demonstrate the use of *Tfu*-FNO as a recycling method for catalytic amounts of several artificial nicotinamide biomimetics in ene-reductase-catalyzed conversions.

To demonstrate the potential use of these thermostable *Tfu*-FNO variants as NCB recycling systems at high temperatures, we measured the activity of a selection of variants toward 5 mM of AmNA$^+$, BNA$^+$, and BAP$^+$ at both 25 and 50 °C. Gratifyingly, the performance increased at elevated temperature. This makes *Tfu*-FNO variants especially suitable for NCB recycling methods for conversions at relatively high temperatures (see Figure 2B).

DISCUSSION

Nicotinamide-dependent oxidoreductases make up one-third of all redox enzymes and are of paramount importance in biocatalysis. The stability and cost of NAD(P), however, make these compounds less attractive for green chemistry.[7,8] Therefore, a range of artificial biomimetics were introduced as alternative nicotinamide cofactors. These small 1- and 3-substituted pyridines were first introduced for mechanistic studies and thereafter also proved their value as stable and low-cost cofactors.[7−9] Many NCBs have a lower redox potential in comparison to their natural counterparts as an additional benefit. The challenge with these NCBs, however, is proper cofactor recycling of the reduced form. Several metal-based catalysts have been proposed as recycling agents,[31,35] which are hard to reconcile with white biotechnology.

The low redox potential of these artificial cofactors and their non-natural structure make it hard to find efficient enzyme-mediated recycling systems. The naturally occurring cofactor F_{420}, which is found in a plethora of archaea and actinobacteria,[46] has a compatibly low redox potential (−360 mV) with many of these NCBs.[13] This makes the cofactor suitable for use in NCB recycling systems. In fact, we could indeed show for the thermostable F_{420}:NADPH oxidoreductase from *T. fusca*, which naturally catalyzes the hydride transfer between the redox pairs $F_{420}/F_{420}H_2$ and NADP$^+$/NADPH, that it is also able to reduce a range of nicotinamide biomimetics (see Figure 1 and Table 1). In fact, this is, to the best of our knowledge, the first study to consider such a large and diverse array of artificial nicotinamides. Although the wild-type FNO activity toward these NCBs is relatively low, we could show that several structure-inspired variants with single amino acid substitutions at positions 29 and 89 have drastically increased reduction rates for several NCBs. Especially the G29W variant, which has a 139 times increase in catalytic efficiency toward 1-benzylnicotinamide (BNA$^+$) in comparison to wild-type *Tfu*-FNO, has a k_{cat} value for 1-benzyl-3-acetylpyridine (DAP$^+$) that is similar to the wild-type activity toward the native substrate NADP$^+$.[40] To the best of our knowledge, this *Tfu*-FNO variant is in fact the best recycling catalyst for BNA$^+$ and BAP$^+$ reported thus far (see Table 2). The reduced forms of these NCBs are especially interesting for the reduction of α,β-unsaturated carbonyl compounds, as they were shown to outperform NADPH as a reducing agent for several ene-reductases.[22]

Table 2. Turnover Numbers for the Reduction of BNA$^+$ and BAP$^+$ for Several Recycling Systems

	turnover number (min^{-1})	
recycling catalyst	BNA$^+$	BAP$^+$
Tfu-FNO G29W	25	252
*Ss*GDH I192T/V306I[45]	0.54	
[Cp*Rh(bpy)H]$^+$[26]	0.15	0.15
ATHase IrC-Sav S112K[30]	4.0	
ATHase IrC-Sav No Sav[30]	7.2	

We could show that variants P89H, G29Y, and G29W are indeed efficient NCB recycling systems in bioconversions, in combination with an ene-reductase. Only a catalytic amount of 1 mM of NCB was necessary to convert 5−10 mM ketoisophorone within 16 h. Not only F_{420} but also its artificial biomimetic FOP[14] could be used for these conversions. The use of FOP might overcome the upscaling problems that F_{420} could face, as thus far it needs to be isolated from slow-growing organisms.[42]

The catalytic activity toward the native substrate, NADP$^+$, was drastically decreased for most of the variants that are described in this study. Therefore, these *Tfu*-FNO variants could also be employed as biorthogonal systems in parallel with NAD(P)-dependent systems, when one or several additional mutations are introduced that completely inhibit NADP$^+$ binding. Kumar et al. have already shown that they could drastically decrease the catalytic efficiency for the natural substrate by introducing single or several point mutations at positions that would not interfere with NCB binding.[40]

https://doi.org/10.1021/acscatal.1c03033
ACS Catal. 2021, 11, 11561−11569

In this study the F_{420}-dependent glucose-6-phosphate dehydrogenase from *R. jostii* RHA1 (FGD-RHA1) and the F_{420}-dependent sugar-6-phosphate dehydrogenase from *C. arvum* (FSD-Cryar) were used as recycling enzymes in the conversion experiments as a proof of concept, which use the somewhat expensive sacrificial electron donor glucose-6-phosphate. For industrial applications other cheaper and more accessible electron donors might be used, such as isopropanol, formate, or hydrogen gas in combination with F_{420}-dependent alcohol dehydrogenases or formate dehydrogenases or hydrogenases, respectively.[47−52] The use of these electron donors could make this an inexpensive and scalable recycling system.

Moreover, the thermostability of the *Tfu*-FNO variants make them lucrative for high-temperature conversions. Not only are they stable at elevated temperatures but they were also shown to have greater NCB reduction rates when they were used at 50 °C, in comparison to room temperature. Thermostability often also ensures organic cosolvent tolerance, which would also make this NCB recycling method ideal for processes that involve highly hydrophobic compounds.

The toolbox of F_{420}:NADPH oxidoreductases that were tailor-made to accept NCBs, as presented in this study, could make the application of NAD(P)-dependent oxidoreductases in large-scale biocatalysis more feasible. These thermostable enzymes can be implemented as efficient enzymatic recycling systems for catalytic amounts of NCBs at ambient and elevated temperatures, harnessing the reductive power of F_{420} and FOP.

■ ASSOCIATED CONTENT

Supporting Information

The Supporting Information is available free of charge at https://pubs.acs.org/doi/10.1021/acscatal.1c03033.

A list of mutagenic primers used to engineer *Tfu*-FNO and graphs of the activity measurements (PDF)

■ AUTHOR INFORMATION

Corresponding Author

Marco W. Fraaije − *Molecular Enzymology Group, University of Groningen, 9747AG Groningen, The Netherlands;* orcid.org/0000-0001-6346-5014; Email: m.w.fraaije@rug.nl

Authors

Jeroen Drenth − *Molecular Enzymology Group, University of Groningen, 9747AG Groningen, The Netherlands*

Guang Yang − *Molecular Enzymology Group, University of Groningen, 9747AG Groningen, The Netherlands*

Caroline E. Paul − *Department of Biotechnology, Delft University of Technology, 2629HZ Delft, The Netherlands;* orcid.org/0000-0002-7889-9920

Complete contact information is available at: https://pubs.acs.org/10.1021/acscatal.1c03033

Author Contributions

M.W.F., C.E.P. and J.D. designed the project. J.D., G.Y., and C.E.P. designed and performed the experiments and analyzed the results. J.D. and M.W.F. wrote the manuscript.

Author Contributions

[§]J.D. and G.Y. contributed equally to this work

Funding

Funding came from the Dutch research council; NWO (VICI grant).

Notes

The authors declare no competing financial interest.

■ ACKNOWLEDGMENTS

We thank Martijn Deinum for help in experimental work.

■ LIST OF ABBREVIATIONS

$AmNA^+$, 1-aminoethylnicotinamide; BAA^+, 1-benzylnicotinic acid; BAP^+, 1-benzyl-3-acetylpyridine; BNA^+, 1-benzylnicotinamide; $EtNA^+$, 1-ethylnicotinamide; $EtOHNA^+$, 1-hydroxyethylnicotinamide; FGD-RHA1, *Rhodococcus jostii* RHA1 F_{420}-dependent glucose-6-phosphate dehydrogenase; FSD-Cryar, *Cryptosporangium arvum* F_{420}-dependent sugar-6-phosphate dehydrogenase; MNA^+, 1-methylnicotinamide; $ProNA^+$, 1-propylnicotinamide; $ProOHNA^+$, 1-hydroxypropylnicotinamide; *Tfu*-FNO, *Thermobifida fusca* F_{420}:NADPH oxidoreductase; *Ts*OYE, *Thermus scotoductus* ene-reductase

■ REFERENCES

(1) Hughes, D. L. Biocatalysis in Drug Development - Highlights of the Recent Patent Literature. *Org. Process Res. Dev.* **2018**, *22* (9), 1063−1080.

(2) Hecht, K.; Meyer, H.-P.; Wohlgemuth, R.; Buller, R. Biocatalysis in the Swiss Manufacturing Environment. *Catalysts* **2020**, *10* (12), 1420.

(3) Buller, R.; Hecht, K.; Mirata, M. A.; Meyer, H. P. CHAPTER 1: An Appreciation of Biocatalysis in the Swiss Manufacturing Environment. In *RSC Catalysis Series*; Royal Society of Chemistry: 2018; Vol. *2018-January*, pp 3−43. DOI: 10.1039/9781782629993-00001.

(4) Schomburg, I.; Jeske, L.; Ulbrich, M.; Placzek, S.; Chang, A.; Schomburg, D. The BRENDA Enzyme Information System-From a Database to an Expert System. *J. Biotechnol.* **2017**, *261*, 194−206.

(5) Sellés Vidal, L.; Kelly, C. L.; Mordaka, P. M.; Heap, J. T. Review of NAD(P)H-Dependent Oxidoreductases: Properties, Engineering and Application. *Biochim. Biophys. Acta, Proteins Proteomics* **2018**, *1866*, 327−347.

(6) Wu, H.; Tian, C.; Song, X.; Liu, C.; Yang, D.; Jiang, Z. Methods for the Regeneration of Nicotinamide Coenzymes. *Green Chem.* **2013**, *15*, 1773−1789.

(7) Wu, J. T.; Wu, L. H.; Knight, J. A. Stability of NADPH: Effect of Various Factors on the Kinetics of Degradation. *Clin. Chem.* **1986**, *32* (2), 314−319.

(8) Paul, C. E.; Arends, I. W. C. E.; Hollmann, F. Is Simpler Better? Synthetic Nicotinamide Cofactor Analogues for Redox Chemistry. *ACS Catal.* **2014**, *4* (3), 788−797.

(9) Norris, D. J.; Stewart, R. Synthesis of a Series of Substituted Pyridinium Ions and Their 1,4-Dihydro Reduction Products and a Determination of Their Stabilities in Aqueous Buffers. *Can. J. Chem.* **1977**, *55*, 1687−1695.

(10) Knox, R. J.; Jenkins, T. C.; Hobbs, S. M.; Chen, S.; Melton, R. G.; Burke, P. J. Bioactivation of 5-(Aziridin-1-Yl)-2,4-Dinitrobenzamide (CB 1954) by Human NAD(P)H Quinone Oxidoreductase 2: A Novel Co-Substrate-Mediated Antitumor Prodrug Therapy. *Cancer Res.* **2000**, *60* (15), 4179−4186.

(11) Paul, C. E.; Hollmann, F. A Survey of Synthetic Nicotinamide Cofactors in Enzymatic Processes. *Appl. Microbiol. Biotechnol.* **2016**, *100*, 4773−4778.

(12) Wolfe, R. S.; Vogels, G. D.; Eirich, L. D. Proposed Structure for Coenzyme F_{420} from *Methanobacterium*. *Biochemistry* **1978**, *17* (22), 4583−4593.

(13) Walsh, C. Naturally Occurring 5-Deazaflavin Coenzymes: Biological Redox Roles. *Acc. Chem. Res.* **1986**, *19* (7), 216−221.

(14) Drenth, J.; Trajkovic, M.; Fraaije, M. W. Chemoenzymatic Synthesis of an Unnatural Deazaflavin Cofactor That Can Fuel F_{420}-Dependent Enzymes. *ACS Catal.* **2019**, *9* (7), 6435.
(15) Friedlos, F.; Jarman, M.; Davies, L. C.; Boland, M. P.; Knox, R. J. Identification of Novel Reduced Pyridinium Derivatives as Synthetic Co-Factors for the Enzyme DT Diaphorase (NAD(P)H Dehydrogenase (Quinone), EC 1.6.99.2). *Biochem. Pharmacol.* **1992**, *44* (1), 25−31.
(16) Knox, R. J.; Friedlos, F.; Jarman, M.; Davies, L. C.; Goddard, P.; Anlezark, G. M.; Melton, R. G.; Sherwood, R. F. Virtual Cofactors for an Escherichia Coli Nitroreductase Enzyme: Relevance to Reductively Activated Prodrugs in Antibody Directed Enzyme Prodrug Therapy (ADEPT). *Biochem. Pharmacol.* **1995**, *49* (11), 1641−1647.
(17) Ryan, J. D.; Fish, R. H.; Clark, D. S. Engineering Cytochrome P450 Enzymes for Improved Activity towards Biomimetic 1,4-NADH Cofactors. *ChemBioChem* **2008**, *9* (16), 2579−2582.
(18) Lutz, J.; Hollmann, F.; Ho, T. V.; Schnyder, A.; Fish, R. H.; Schmid, A. Bioorganometallic Chemistry: Biocatalytic Oxidation Reactions with Biomimetic NAD^+/NADH Co-Factors and $[Cp^*Rh(Bpy)H]^+$ for Selective Organic Synthesis. *J. Organomet. Chem.* **2004**, *689* (25), 4783−4790.
(19) Guarneri, A.; Westphal, A. H.; Leertouwer, J.; Lunsonga, J.; Franssen, M. C. R.; Opperman, D. J.; Hollmann, F.; van Berkel, W. J. H.; Paul, C. E. Flavoenzyme-Mediated Regioselective Aromatic Hydroxylation with Coenzyme Biomimetics. *ChemCatChem* **2020**, *12* (5), 1368−1375.
(20) Qi, J.; Paul, C. E.; Hollmann, F.; Tischler, D. Changing the Electron Donor Improves Azoreductase Dye Degrading Activity at Neutral PH. *Enzyme Microb. Technol.* **2017**, *100*, 17−19.
(21) Paul, C. E.; Gargiulo, S.; Opperman, D. J.; Lavandera, I.; Gotor-Fernández, V.; Gotor, V.; Taglieber, A.; Arends, I. W. C. E.; Hollmann, F. Mimicking Nature: Synthetic Nicotinamide Cofactors for C = C Bioreduction Using Enoate Reductases. *Org. Lett.* **2013**, *15* (1), 180−183.
(22) Knaus, T.; Paul, C. E.; Levy, C. W.; De Vries, S.; Mutti, F. G.; Hollmann, F.; Scrutton, N. S. Better than Nature: Nicotinamide Biomimetics That Outperform Natural Coenzymes. *J. Am. Chem. Soc.* **2016**, *138* (3), 1033−1039.
(23) Löw, S. A.; Löw, I. M.; Weissenborn, M. J.; Hauer, B. Enhanced Ene-Reductase Activity through Alteration of Artificial Nicotinamide Cofactor Substituents. *ChemCatChem* **2016**, *8* (5), 911−915.
(24) Riedel, A.; Mehnert, M.; Paul, C. E.; Westphal, A. H.; van Berkel, W. J. H.; Tischler, D. Functional Characterization and Stability Improvement of a 'Thermophilic-like' Ene-Reductase from Rhodococcus Opacus 1CP. *Front. Microbiol.* **2015**, *6*, 1073.
(25) Geddes, A.; Paul, C. E.; Hay, S.; Hollmann, F.; Scrutton, N. S. Donor-Acceptor Distance Sampling Enhances the Performance of "Better than Nature" Nicotinamide Coenzyme Biomimetics. *J. Am. Chem. Soc.* **2016**, *138* (35), 11089−11092.
(26) Lo, H. C.; Fish, R. H. Biomimetic NAD^+ Models for Tandem Cofactor Regeneration, Horse Liver Alcohol Dehydrogenase Recognition of 1,4-NADH Derivatives, and Chiral Synthesis. *Angew. Chem., Int. Ed.* **2002**, *41* (3), 478−481.
(27) Fish, R. H. 1,4-NADH Biomimetic Co-Factors with Horse Liver Alcohol Dehydrogenase (HLADH), Utilizing $[Cp^*Rh(Bpy)H](OTf)$ for Co-Factor Regeneration, Do in Fact, Produce Chiral Alcohols from Reactions with Achiral Ketones. *Catalysts* **2019**, *9* (6), 562.
(28) Josa-Culleré, L.; Lahdenperä, A.; Ribaucourt, A.; Höfler, G.; Gargiulo, S.; Liu, Y.-Y.; Xu, J.-H.; Cassidy, J.; Paradisi, F.; Opperman, D.; Hollmann, F.; Paul, C. Synthetic Biomimetic Coenzymes and Alcohol Dehydrogenases for Asymmetric Catalysis. *Catalysts* **2019**, *9* (3), 207.
(29) Nowak, C.; Beer, B.; Pick, A.; Roth, T.; Lommes, P.; Sieber, V. A Water-Forming NADH Oxidase from Lactobacillus Pentosus Suitable for the Regeneration of Synthetic Biomimetic Cofactors. *Front. Microbiol.* **2015**, *6*, 957.
(30) Jia, H. Y.; Zong, M. H.; Zheng, G. W.; Li, N. Myoglobin-Catalyzed Efficient in Situ Regeneration of NAD(P) + and Their Synthetic Biomimetic for Dehydrogenase-Mediated Oxidations. *ACS Catal.* **2019**, *9* (3), 2196−2202.
(31) Lo, H. C.; Leiva, C.; Buriez, O.; Kerr, J. B.; Olmstead, M. M.; Fish, R. H. Bioorganometallic Chemistry. 13. Regioselective Reduction of NAD^+ Models, 1-Benzylnicotinamde Triflate and b-Nicotinamide Ribose-5′-Methyl Phosphate, with in Situ Generated $[Cp^*Rh(Bpy)H]^+$: Structure-Activity Relationships, Kinetics, and Mechanistic Aspects in the Formation of the 1,4-NADH Derivatives. *Inorg. Chem.* **2001**, *40*, 6705−6716.
(32) Knaus, T.; Paul, C. E.; Levy, C. W.; De Vries, S.; Mutti, F. G.; Hollmann, F.; Scrutton, N. S. Better than Nature: Nicotinamide Biomimetics That Outperform Natural Coenzymes. *J. Am. Chem. Soc.* **2016**, *138* (3), 1033−1039.
(33) Hildebrand, F.; Lütz, S. Stable Electroenzymatic Processes by Catalyst Separation. *Chem. - Eur. J.* **2009**, *15* (20), 4998−5001.
(34) Kim, J.; Lee, S. H.; Tieves, F.; Choi, D. S.; Hollmann, F.; Paul, C. E.; Park, C. B. Biocatalytic C = C Bond Reduction through Carbon Nanodot-Sensitized Regeneration of NADH Analogues. *Angew. Chem., Int. Ed.* **2018**, *57* (42), 13825−13828.
(35) Okamoto, Y.; Köhler, V.; Paul, C. E.; Hollmann, F.; Ward, T. R. Efficient in Situ Regeneration of NADH Mimics by an Artificial Metalloenzyme. *ACS Catal.* **2016**, *6* (6), 3553−3557.
(36) Nowak, C.; Pick, A.; Lommes, P.; Sieber, V. Enzymatic Reduction of Nicotinamide Biomimetic Cofactors Using an Engineered Glucose Dehydrogenase: Providing a Regeneration System for Artificial Cofactors. *ACS Catal.* **2017**, *7* (8), 5202−5208.
(37) Huang, R.; Chen, H.; Upp, D. M.; Lewis, J. C.; Zhang, Y.-H. P. J. A High-Throughput Method for Directed Evolution of NAD(P) + -Dependent Dehydrogenases for the Reduction of Biomimetic Nicotinamide Analogues. *ACS Catal.* **2019**, *9*, 11709−11719.
(38) Cheeseman, P.; Toms-Wood, A.; Wolfe, R. S. Isolation and Properties of a Fluorescent Compound, Factor420, from *Methanobacterium* Strain M.o.H. *J. Bacteriol.* **1972**, *112* (1), 527−531.
(39) Greening, C.; Ahmed, F. H.; Mohamed, A. E.; Lee, B. M.; Pandey, G.; Warden, A. C.; Scott, C.; Oakeshott, J. G.; Taylor, M. C.; Jackson, C. J. Physiology, Biochemistry, and Applications of F420-and Fo-Dependent Redox Reactions. *Microbiol. Mol. Biol. Rev.* **2016**, *80* (2), 451−493.
(40) Kumar, H.; Nguyen, Q. T.; Binda, C.; Mattevi, A.; Fraaije, M. W. Isolation and Characterization of a Thermostable F420:NADPH Oxidoreductase from Thermobifida Fusca. *J. Biol. Chem.* **2017**, *292* (24), 10123−10130.
(41) Bashiri, G.; Rehan, A. M.; Greenwood, D. R.; Dickson, J. M. J.; Baker, E. N. Metabolic Engineering of Cofactor F420 Production in Mycobacterium Smegmatis. *PLoS One* **2010**, *5* (12), No. e15803.
(42) Isabelle, D.; Simpson, D. R.; Daniels, L. Large-Scale Production of Coenzyme F_{420}-5,6 by Using *Mycobacterium Smegmatis*. *Appl. Environ. Microbiol.* **2002**, *68* (11), 5750−5755.
(43) Nguyen, Q.-T.; Trinco, G.; Binda, C.; Mattevi, A.; Fraaije, M. W. Discovery and Characterization of an F_{420}-Dependent Glucose-6-Phosphate Dehydrogenase (Rh-FGD1) from *Rhodococcus Jostii* RHA1. *Appl. Microbiol. Biotechnol.* **2017**, *101* (7), 2831−2842.
(44) Mascotti, M. L.; Kumar, H.; Nguyen, Q. T.; Ayub, M. J.; Fraaije, M. W. Reconstructing the Evolutionary History of F420-Dependent Dehydrogenases. *Sci. Rep.* **2018**, *8* (1), 17571.
(45) Opperman, D. J.; Sewell, B. T.; Litthauer, D.; Isupov, M. N.; Littlechild, J. A.; van Heerden, E. Crystal Structure of a Thermostable Old Yellow Enzyme from Thermus Scotoductus SA-01. *Biochem. Biophys. Res. Commun.* **2010**, *393* (3), 426−431.
(46) Ney, B.; Ahmed, F. H.; Carere, C. R.; Biswas, A.; Warden, A. C.; Morales, S. E.; Pandey, G.; Watt, S. J.; Oakeshott, J. G.; Taylor, M. C.; Stott, M. B.; Jackson, C. J.; Greening, C. The Methanogenic Redox Cofactor F_{420} Is Widely Synthesized by Aerobic Soil Bacteria. *ISME J.* **2017**, *11* (1), 125−137.
(47) Aufhammer, S. W.; Warkentin, E.; Berk, H.; Shima, S.; Thauer, R. K.; Ermler, U. Coenzyme Binding in F_{420}-Dependent Secondary Alcohol Dehydrogenase, a Member of the Bacterial Luciferase Family. *Structure* **2004**, *12* (3), 361−370.

https://doi.org/10.1021/acscatal.1c03033
ACS Catal. 2021, 11, 11561−11569

(48) Schauer, N. L.; Ferry, J. G.; Honek, J. F.; Orme-Johnson, W. H.; Walsh, C. Mechanistic Studies of the Coenzyme F420Reducing Formate Dehydrogenase from Methanobacterium Formicicum. *Biochemistry* **1986**, 25 (22), 7163−7168.
(49) Thauer, R. K.; Kaster, A. K.; Goenrich, M.; Schick, M.; Hiromoto, T.; Shima, S. Hydrogenases from Methanogenic Archaea, Nickel, a Novel Cofactor, and H2 Storage. *Annu. Rev. Biochem.* **2010**, *79*, 507−536.
(50) Schauer, N. L.; Ferry, J. G. Composition of the Coenzyme F_{420}-Dependent Formate Dehydrogenase from *Methanobacterium Formicicum*. *J. Bacteriol.* **1986**, *165* (2), 405−411.
(51) Vitt, S.; Ma, K.; Warkentin, E.; Moll, J.; Pierik, A. J.; Shima, S.; Ermler, U. The F_{420}-Reducing [NiFe]-Hydrogenase Complex from *Methanothermobacter Marburgensis*, the First X-Ray Structure of a Group 3 Family Member. *J. Mol. Biol.* **2014**, *426* (15), 2813−2826.
(52) Martin, C.; Tjallinks, G.; Trajkovic, M.; Fraaije, M. Facile Stereoselective Reduction of Prochiral Ketones by Using an F_{420}-Dependent Alcohol Dehydrogenase. *ChemBioChem* **2021**, *22* (1), 156−159.

https://doi.org/10.1021/acscatal.1c03033
ACS Catal. 2021, 11, 11561−11569